下扬子地区姚村A型花岗岩年代学、地球化学特征及岩石成因

王存智[1],黄志忠[1],赵希林[1],褚平利[1],黄文成[1],宋世明[1],徐杨[2],杨超[3]

(1.中国地质调查局南京地质调查中心,江苏 南京 210016;2.中国地质调查局武汉地质调查中心,湖北 武汉 430223;3.合肥工业大学资源与环境工程学院,安徽 合肥 230009)

提要:姚村岩体位于下扬子江南造山带东北端,主要由中心相的中粗粒正长花岗岩和边缘相的细粒似斑状正长花岗岩组成。本文对该岩体进行了详细的锆石U−Pb年代学、主量元素、微量元素以及Nd−Hf同位素研究。LA−ICP−MS锆石U−Pb定年表明姚村岩体的形成年龄为(127.6±1.4)Ma,为燕山晚期岩浆活动的产物。岩石地球化学研究表明姚村岩体属于A型花岗岩,具高硅、富铁,锆饱和温度高、轻重稀土分馏明显、富集Rb、Th、U、K、Pb等元素而亏损Ba、Nb、Sr和Ti等元素、铕负异常显著(Eu /Eu*=0.22~0.46)的特点。姚村岩体的全岩 $\varepsilon_{Nd}(t)$ 值与锆石 $\varepsilon_{Hf}(t)$ 值分别变化于 $-6.2 \sim -5.7$ 和 $-13.9 \sim -5.0$,两阶段 Nd 和 Hf 同位素模式年龄分别为 T_{DM2} (Nd)=1439~1532 Ma 和 T_{DM2} (Hf)=1508~2062 Ma,Nd 同位素的模式年龄重叠于 Hf 同位素模式年龄。结合区域地质研究成果认为,姚村岩体可能于早白垩世古太平洋板块俯冲作用之后伸展−拉伸环境下,由中元古代地壳重熔而成。

关　键　词:A型花岗岩;早白垩世;岩石成因;地质调查工程;姚村岩体;下扬子;安徽

中图分类号:P588.12;P597+.3;P595　　　**文献标志码**:A　　**文章编号**:1000−3657(2021)02−0549−15

Geochronology, geochemistry and petrogenesis of early Cretaceous Yaocun A−type granite in the Lower Yangtze region

WANG Cunzhi[1], HUANG Zhizhong[1], ZHAO Xilin[1], CHU Pingli[1], HUANG Wencheng[1], SONG Shiming[1], XU Yang[2], YANG Chao[3]

(1.*Nanjing Center, China Geological Survey, Nanjing* 210016, *Jiangsu, China;* 2. *Wuhan Center, China Geological Survey, Wuhan* 430223, *Hubei, China;* 3. *School of Resources and Environmental Engineering, Hefei University of Technology, Hefei* 230009, *Anhui, China*)

Abstract: The Yaocun pluton in Southern Anhui Province, lithologically consisting mainly of medium− to coarse− grained syenogranite in its centre and fine−grained porphyritic syenogranite on its margin, is outcropped around the northeastern Jiangnan orogeny of the Lower Yangtze region. This paper reports detailed study results of its the LA−ICP−MS zircon U−Pb dating, major elements, trace elements, whole−rock Nd isotopic compositions and zircon Hf isotopic compositions. LA−ICP−MS zircon U−Pb

ages show that the Yaocun pluton, as the product of magmatic activity in the late Yanshanian period, was emplaced at 127.6±1.4Ma. The studies of petrography and geochemistry of this rock indicate that it is A−type granite, and is characterized by rich silica, high iron, high zircon saturation temperatures, enrichment of Rb, Th, U, K and Pb, depletion of Ba, Nb, Sr and Ti, and significant negative Eu anomalies (Eu/Eu*=0.22−0.46). Its $\varepsilon_{Nd}(t)$ and $\varepsilon_{Hf}(t)$ values range from −6.2 to −5.7 and from −13.9 to −5.0 respectively, and the calculated two−stage model ages (T_{DM2}) of Nd and Hf isotopes from 1439 Ma to 1532 Ma and from 1508 Ma to 2062 Ma respectively. Combined with the results of regional geological research, it is suggested that the Yaocun pluton might be formed by the Mesoproterozoic crust remelting under extension−tension environment after the subduction of the Paleo−Pacific plate during the Early Cretaceous.

Key words: A−type granite; Early Cretaceous; petrogenesis; geological survey engineering; Yaocun pluton; Lower Yangtze region; Anhui Province

About the first author: WANG Cunzhi, male, born in 1983, senior engineer, engaged in the study of structural geology; Email: 32107407@qq.com

1 引 言

下扬子地区包括长江中下游和江南造山带两个构造单元(图1a),以广泛发育燕山期岩浆作用为特点。对其中长江中下游地区的研究表明,岩浆事件主要可分为4期:第一期为145~135 Ma,包括发育在断隆区的高钾钙碱性闪长岩类,一般具有埃达克岩特征;第二期为135~128 Ma,以发育在断凹区的橄榄安粗岩系火山岩和双峰式火山岩为主;第三期为127~123 Ma,主要为A型花岗岩;第四期为109~101 Ma,以宁镇地区的中酸性侵入岩为主(毛景文等,2004;周涛发等,2008;闫峻等,2012;薛怀民等,2013;关俊朋等,2015;薛怀民等,2016;王继强等,2017;王存智等,2018;陈俊等,2018)。

江南造山带的燕山期岩浆岩分布更加广泛,近年来大量的高精度年代学资料显示,皖南江南造山带燕山期岩浆活动可分为两期:分别为152~137 Ma和136~122 Ma(Wu et al., 2012;闫峻等,2017)。早期以花岗闪长岩为主,属于高钾钙碱性系列I型花岗岩(薛怀民等,2009;周翔等,2012;Wu et al., 2012;周洁等,2013);晚期以正长花岗岩为主,少量二长花岗岩,多数具有A型花岗岩的特征(薛怀民等,2009;Wu et al., 2012;Zhou et al., 2013;陈芳等,2014;高冉等,2017)。

但是,目前对于皖南江南造山带燕山期岩浆岩的研究多集中在皖南山区,对于北东段的工作明显偏弱,特别是关于姚村岩体的研究,仅有一个较为可靠的年代学资料(Wu et al., 2012)。本次工作对姚村岩体开展了详细的LA-ICP-MS锆石U-Pb定年、全岩主量和微量稀土元素、Nd同位素和锆石Hf同位素组成的研究工作,以深入探讨姚村岩体的岩石成因类型、物质来源及构造环境。

2 地质背景及岩体地质特征

下扬子地区位于扬子板块东部,其北和西北部以襄樊—广济断裂、郯庐断裂为界与大别造山带相邻,南以江绍断裂为界与华夏地块相接。通常以江南断裂为界,下扬子地区又可分为北西的长江中下游地区(沿江带)和南东的皖南江南造山带(江南带)两个构造单元(闫峻等,2017)(图1a)。

姚村岩体位于皖南江南造山带北东段,地理位置处于安徽省郎溪县西南部的姚村乡。研究区内NE向断裂发育,并被少量NW向断裂所切。燕山期岩浆侵入活动强烈,多以中大型岩基或者复式岩体出露,如太平—黄山岩体、九华山岩体、刘村岩体及姚村岩体等(图1b)。

姚村岩体呈北东向椭圆状侵入于志留系砂泥岩中(图1c),出露面积约107 km²。岩体与围岩界线清晰,接触面呈波状或锯齿状,均外倾。接触带热变质作用强烈,形成宽500~1000 m角岩带。岩体边部局部发育宽窄不等的冷凝边,并偶见角岩化的砂岩捕虏体。姚村岩体主要由中心相的中粗粒正长花岗岩和边缘相的细粒似斑状正长花岗岩组成,两者呈渐变过渡关系,晚期还有细粒花岗岩侵入。

中粗粒正长花岗岩呈浅灰-肉红色,块状构造,中粗粒花岗结构(图2a),局部呈似斑状。主要矿物
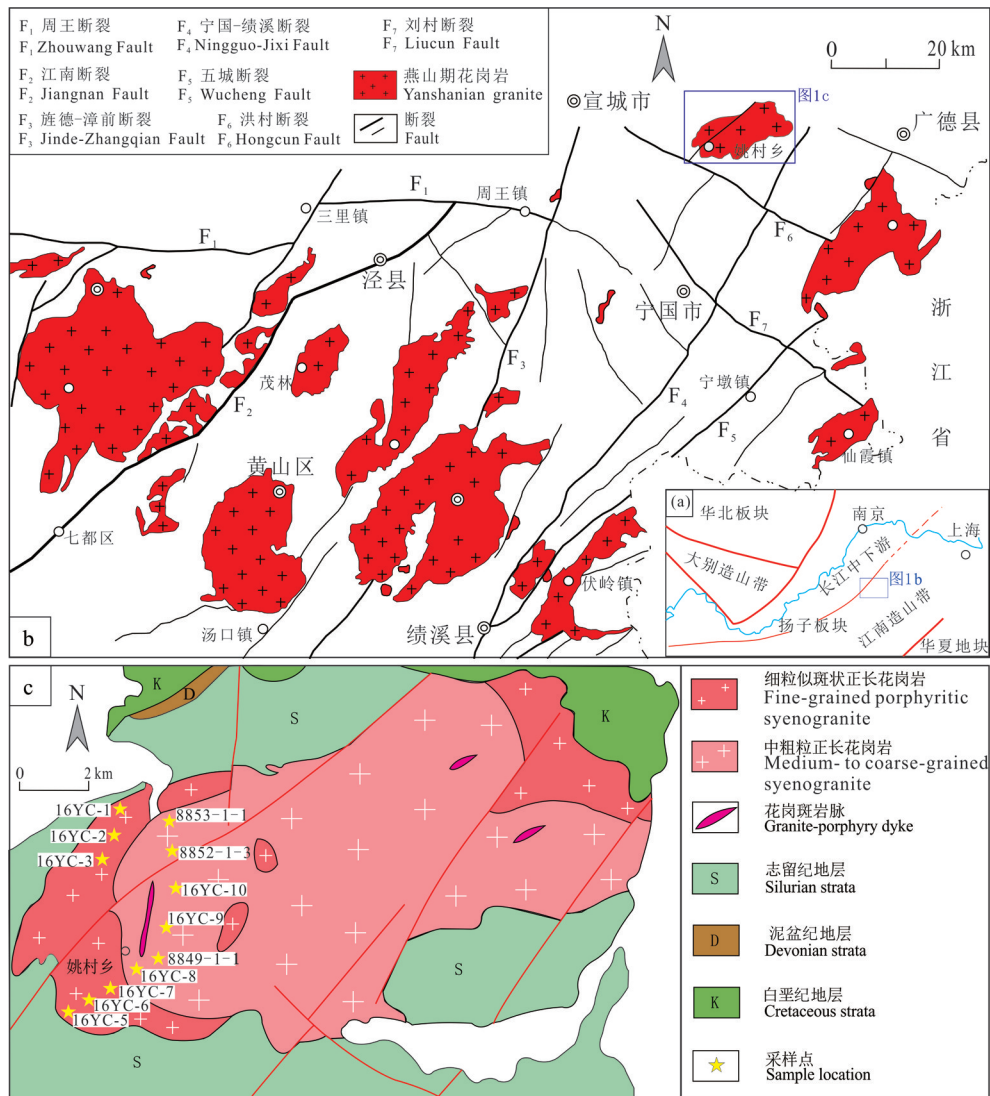
图1 大地构造位置图(a)、区域构造略图(b,据陈芳等,2014修改)及岩体地质简图(c)

Fig.1 Schematic tectonic map of Lower Yangtze region showing the location of the studied area(a) ; tectonic sketch map of the studied area(b,after Chen Fang et al., 2014); and geological sketch map of the Yaocun pluton(c)

成分为石英(30%~35%),斜长石(10%~15%,可见聚片双晶),条纹长石(45%~55%),黑云母(2%~5%)(图2b)。副矿物有锆石、磷灰石、褐帘石等。

细粒似斑状正长花岗岩呈肉红—浅肉红色,块状构造,似斑状结构(图2c)。斑晶以石英为主,次为钾长石。基质呈细粒结构,由条纹长石(45%~50%)、石英(25%~35%)、斜长石(10%~20%)及少量黑云母(2%~5%)组成(图2d)。副矿物有锆石、磷灰石等。

3　分析测试方法

全岩粉末样处理及锆石挑选工作在河北省廊坊辰昌岩矿检测技术服务有限公司进行,锆石制靶及阴极发光(CL)照相在北京锆年领航科技有限公司完成。

全岩主量和微量元素分析在国家地质实验测试中心完成,其中主量元素采用X射线荧光光谱法(XRF)测定(仪器型号:PE300D),并采用等离子光谱和化学法测定进行互检。微量元素和稀土元素采用电感耦合等离子质谱法(ICP-MS)测定(型号:PW4400),同时分析2个国家标样(GSR3和GSR5)和3个平行样以保证分析结果的准确度,分析精度相对误差符合行业标准。

全岩Sr-Nd同位素在核工业北京地质研究院
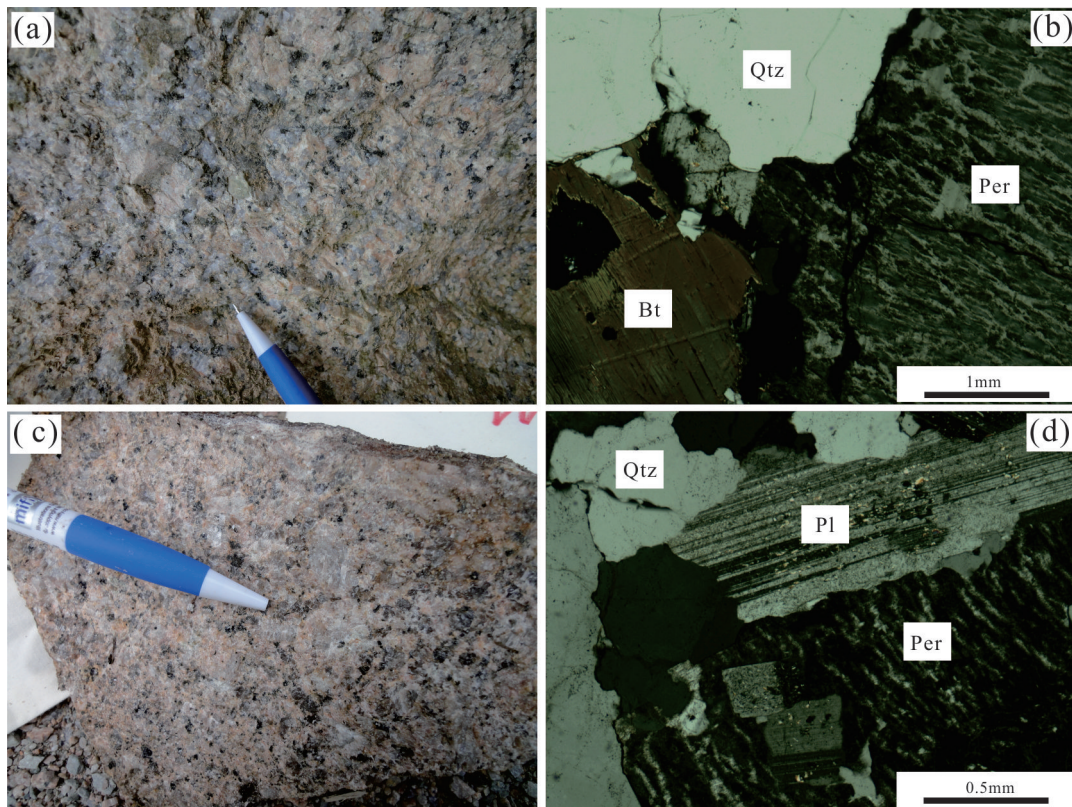
图2 姚村岩体野外及镜下照片
Q—石英；Pl—斜长石；Per—条纹长石；Bi—黑云母
Fig.2 Field and microscope photographs of the Yaocun pluton
Qtz−quartz; Pl−plagioclase; Per−perthite; Bt−biotite

分析测试研究中心完成。根据微量元素中 Rb−Sr、Sm−Nd 含量称取适量样品于 Teflon 闷罐中，加入 $^{87}Rb-^{84}Sr$ 和 $^{149}Sm-^{150}Nd$ 混合稀释剂并用 HF、HNO_3 和 $HClO_4$ 充分溶解后用离子交换树脂分离出 Rb、Sr、Sm 和 Nd，在 ISOPROBE−T 热电离质谱仪（TIMS）上测试。整个分析流程实验本底为：Rb、Sr <$100×10^{-12}$；Sm、Nd <$50×10^{-12}$。

LA−ICP−MS 锆石 U−Pb 定年测试分析在中国地质科学院矿产资源研究所 MC−ICP−MS 实验室完成，锆石定年分析所用仪器为 Finnigan Neptune 型 MC−ICP−MS 及与之配套的 Newwave UP213 激光剥蚀系统。激光剥蚀所用斑束直径为 25 μm，频率为 10 Hz，能量密度约为 2.5 J/cm^2，以 He 为载气。LA−MC−ICP−MS 激光剥蚀采用单点剥蚀的方法，数据分析前用锆石 GJ−1 为外标，U、Th 含量以锆石 M127 为外标进行校正。数据处理采用 ICPMSDataCal 程序（Liu et al., 2008, 2010），锆石年

龄谐和图用 Isoplot3.0 程序获得（Ludwig, 2003）。详细参数及实验测试过程参见侯可军等（2009）。

锆石 Hf 同位素分析测试工作在南京大学内生金属矿床成矿机制研究国家重点实验室完成。该项分析是在锆石 LA−ICP−MS U−Pb 定年的基础上，参照锆石 CL 图像，选择在原年龄测点位置或附近进行，所用仪器为 New−wave UP193 激光剥蚀系统及其相连接的 Thermo Neptune Plus 多接收等离子体质谱仪，以 He 作为载气，分析中使用的激光束斑直径为 44 μm，频率为 8 Hz，剥蚀时间为 26 s，采用 MT 作为外部标样，$^{176}Hf/^{177}Hf$ 比值为 0.282530±0.000030。$ε_{Hf}(t)$ 计算采用的 ^{176}Lu 的衰变常数为 $1.865×10^{-11}$（Scherer et al., 2001），球粒陨石 $^{176}Hf/^{177}Hf$=0.282772，$^{176}Lu/^{177}Hf$=0.0332（Blichert, 1997）。亏损地幔 Hf 模式年龄（T_{DM1}）采用 $^{176}Hf/^{177}Hf$=0.283251，$^{176}Lu/^{177}Hf$=0.0384（Vervoot & Blichert−Toft, 1999），二阶段 Hf 模式年龄（T_{DM2}）采用平均大

陆壳 $^{176}Lu/^{177}Hf=0.015$ 计算（Griffin et al., 2002）。

4 分析结果

4.1 锆石U-Pb年龄

对姚村岩体中的中粗粒正长花岗岩（8849-1-1）进行了锆石U-Pb年代学研究。样品中锆石呈无色和淡黄色，形态为柱状，长100~120 μm，宽50~60 μm，长宽比一般在2:1左右。在锆石阴极发光图像（CL）上（图3a），所有锆石均发育清晰的震荡环带，显示岩浆锆石的特点。对样品进行了24个点的锆石U-Th-Pb同位素分析，定年数据列于表1。

这些锆石中Pb含量较低，变化于 $2×10^{-6}~10×10^{-6}$，Th含量介于 $58×10^{-6}~306×10^{-6}$，U含量介于 $89×10^{-6}~372×10^{-6}$。Th/U 比值为 0.60~1.06，均大于 0.40，属典型的岩浆成因锆石（Wu and Zheng, 2004）。从测试结果看，样品 $^{206}Pb/^{238}U$ 表面年龄都较为集中，24个点全部集中在125~135 Ma。但部分点（如 1、2、3、4、5、12、13、19、22） $^{207}Pb/^{206}Pb$ 年龄与 $^{206}Pb/^{238}U$ 相差太大，谐和度小于90%，除掉这9个不谐和的数据点外，其他15个点的分析数据在谐和曲线上成群分布（图3b）， $^{206}Pb/^{238}U$ 加权平均年龄为（127.6 ±1.4）Ma（ $n=15$，MSWD=0.31），代表了姚村岩体的形成时代，属早白垩世岩浆活动的产物。

4.2 全岩地球化学特征

对姚村岩体细粒似斑状正长花岗岩和中粗粒正长花岗岩进行了全岩主量、微量和稀土元素分析，结果列于表2。姚村岩体均具有较高的 SiO_2（75.46%~77.55%）和全碱（ Na_2O+K_2O）含量（8.11%~8.75%），较低的 TiO_2（0.08%~0.22%）、CaO（0.23%~0.65%）、MgO（0.07%~0.29%）和 P_2O_5（0.01%~0.04%）含量。在TAS分类图解中（图4a），所有样品全部投入花岗岩区域内，属亚碱性系列。在 SiO_2-K_2O 图解中（图4b），全部落入高钾钙碱性系列。 Al_2O_3 含量为11.85%~12.83%（平均12.42%），铝碱比（A/NK）介于1.08~1.18，铝过饱和度（A/CNK）为1.0~1.1，属弱过铝质岩石。

姚村岩体REE总量为 $125×10^{-6}~241×10^{-6}$，在球粒陨石标准化的稀土元素分布图上（图5a），姚村岩体轻重稀土分馏明显，表现为LREE富集的右倾分布型式，轻重稀土明显分馏，(La/Yb)$_N$=6.40~10.74（平均值为9.46），并且显示强烈的 Eu 负异常（Eu/Eu*=0.22~0.46）。在微量元素原始地幔标准化蛛网图上（图5b），所有样品具有明显的 Rb、U、Th、K、Pb、Nd、Zr、Hf 正异常，显著的 Ba、Nb、Ta、Sr、P、Ti 负异常。

4.3 全岩Sr-Nd同位素和锆石Hf同位素特征

姚村岩体中粗粒正长花岗全岩 Sr、Nd 同位素测试结果列于表3。结果显示，姚村岩体具有均一的 Sr、Nd 同位素组成， $^{87}Sr/^{86}Sr$ 初始比值介于0.7098~0.7101， $^{143}Nd/^{144}Nd$ 值介于 0.512207~
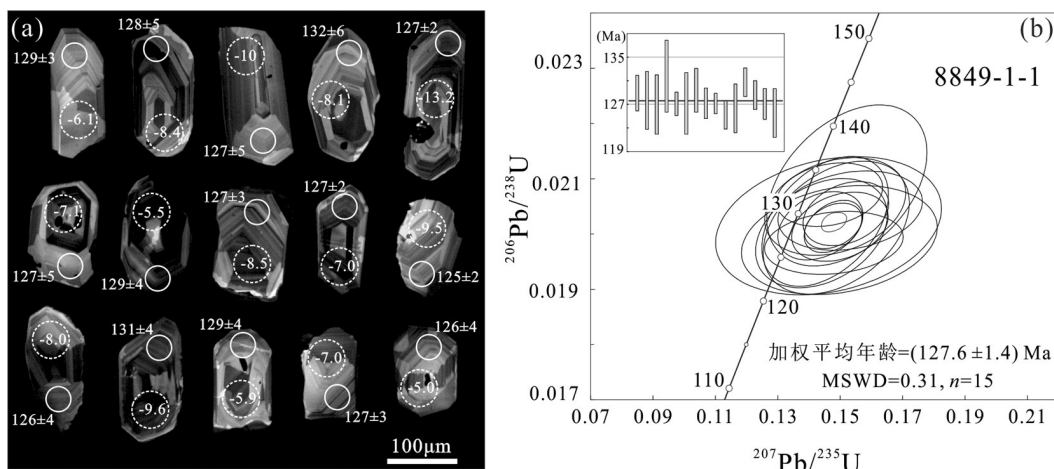

图3 姚村岩体代表性锆石CL图像（a）及U-Pb年龄谐和图（b）
（实线小圈为锆石U-Pb同位素分析点，虚线大圈为Hf同位素分析点）
Fig.3 Cathodoluminescence (CL) images of representative zircons(a) and U-Pb Concordia diagrams of samples(b) from the Yaocun A-type granitic pluton. Small solid circles are spots for U-Pb isotope analyses, and big dashed circles are spots for Hf isotope analyses

表1 姚村岩体中粗粒正长花岗岩(8849-1-1)LA-ICP-MS锆石U-Th-Pb同位素分析结果

Table 1 Zircon LA-ICP-MS U – Pb geochronology results in the Yaocun coarse-grained syenogranite

点号	元素含量/10⁻⁶			Th/U	同位素比值						同位素年龄/Ma				谐和度/%
	Pb	Th	U		$^{207}Pb/^{206}Pb$	1σ	$^{207}Pb/^{235}U$	1σ	$^{206}Pb/^{238}U$	1σ	$^{207}Pb/^{206}Pb$	1σ	$^{206}Pb/^{238}U$	1σ	
8849-1-1-1	2	80	89	0.89	0.0878	0.0052	0.2383	0.0120	0.0212	0.0005	1377	115	132	3	53
8849-1-1-2	3	105	112	0.94	0.0806	0.0038	0.2181	0.0102	0.0208	0.0004	1211	93	130	3	59
8849-1-1-3	4	128	141	0.91	0.0697	0.0052	0.1859	0.0127	0.0204	0.0005	918	149	127	3	71
8849-1-1-4	3	61	102	0.60	0.0795	0.0051	0.2142	0.0127	0.0208	0.0005	1183	128	130	3	60
8849-1-1-5	2	58	92	0.63	0.0878	0.0043	0.2429	0.0122	0.0212	0.0004	1377	127	132	3	51
8849-1-1-6	6	145	220	0.66	0.0526	0.0047	0.1532	0.0153	0.0207	0.0005	309	201	129	3	90
8849-1-1-7	10	306	372	0.82	0.0526	0.0051	0.1452	0.0134	0.0205	0.0008	322	218	128	5	94
8849-1-1-8	4	141	161	0.88	0.0550	0.0070	0.1487	0.0155	0.0204	0.0008	413	285	127	5	91
8849-1-1-9	4	132	153	0.86	0.0554	0.0068	0.1522	0.0169	0.0211	0.0010	428	276	132	6	93
8849-1-1-10	7	196	294	0.67	0.0536	0.0024	0.1478	0.0062	0.0204	0.0003	354	100	127	2	92
8849-1-1-11	6	169	213	0.79	0.0569	0.0116	0.1463	0.0239	0.0204	0.0008	500	387	127	5	93
8849-1-1-12	2	75	96	0.78	0.0908	0.0057	0.2308	0.0122	0.0202	0.0004	1444	120	126	3	51
8849-1-1-13	3	107	125	0.86	0.0937	0.0056	0.2484	0.0122	0.0208	0.0004	1503	114	129	3	48
8849-1-1-14	8	279	296	0.94	0.0528	0.0053	0.1484	0.0149	0.0207	0.0006	320	264	129	4	94
8849-1-1-15	6	206	214	0.96	0.0527	0.0032	0.1437	0.0090	0.0204	0.0003	317	141	127	3	95
8849-1-1-16	9	316	347	0.91	0.0532	0.0021	0.1478	0.0061	0.0204	0.0003	339	89	127	2	92
8849-1-1-17	6	206	234	0.88	0.0532	0.0051	0.1480	0.0147	0.0201	0.0004	339	218	125	2	91
8849-1-1-18	7	278	263	1.06	0.0527	0.0059	0.1440	0.0139	0.0203	0.0007	317	254	126	4	94
8849-1-1-19	4	116	172	0.68	0.0647	0.0041	0.1734	0.0095	0.0207	0.0002	765	133	129	2	79
8849-1-1-20	7	221	247	0.89	0.0512	0.0040	0.1466	0.0113	0.0210	0.0004	250	180	131	2	96
8849-1-1-21	7	211	271	0.78	0.0555	0.0035	0.1518	0.0091	0.0206	0.0004	432	139	129	2	91
8849-1-1-22	3	98	103	0.96	0.0851	0.0044	0.2340	0.0120	0.0210	0.0002	1318	100	131	2	54
8849-1-1-23	5	157	207	0.76	0.0543	0.0038	0.1499	0.0102	0.0204	0.0004	383	192	127	3	91
8849-1-1-24	7	213	252	0.85	0.0538	0.0071	0.1497	0.0207	0.0201	0.0007	361	300	126	4	90

0.512253，$\varepsilon_{Nd}(t)$值变化于-6.2~ -5.7，二阶段Nd模式年龄T_{DM2}介于1493~1532 Ma。

姚村岩体中的中粗粒正长花岗岩(8849-1-1)锆石Hf同位素分析结果列于表4。这些岩浆锆石具有相对均一的Hf同位素组成，$^{176}Lu/^{177}Hf$和$^{176}Hf/^{177}Hf$比值范围较大，分别变化于0.000949~0.001992和0.282303~0.282552，$^{176}Hf/^{177}Hf$初始比值介于0.282299~0.282548，$\varepsilon_{Hf}(t)$值介于-13.9~-5，T_{DM1}介于1004~1364 Ma.，T_{DM2}介于1508~2062 Ma。

5 讨　论

5.1 姚村岩体的成岩年龄

对于姚村岩体的成岩年龄，前人Rb-Sr法曾测得127 Ma的年龄结果(章邦栋，1989)，Wu et al.(2012)也获得正长花岗斑岩LA-ICP-MS锆石U-Pb年龄为(127.2±1.9)Ma。本次获得的姚村岩体似斑状正长花岗岩(8849-1-1)锆石U-Pb年龄为(127.6 ±1.4) Ma，与前人结果在误差范围内一致，代表了姚村岩体的成岩时代。因此，姚村岩体属于皖南江南造山带燕山期岩浆活动的晚阶段，和带内其他A型花岗岩的侵入时代一致。

5.2 岩石类型

根据不同的源岩性质一般将花岗岩被分为I型、S型、M型(Whalen et al.，1987; Bonin, 2007)。而A型花岗岩最先由Loiselle和Wones(1979)提出，用来定义一类碱性(Alkaline)、无水(Anhydrous)、非造山(Anorogenic)的花岗岩，具有特殊的地球化学特征(Loiselle & Wones, 1979)。

姚村岩体具有较高的(Na_2O+K_2O)含量(8.11%~8.75%)、$FeO^T/(FeO^T+MgO)$比值(0.84~0.92)、高场强元素和稀土元素含量，同时具有较低的Ba、Sr、Ti和Eu含量，这些地球化学特征与典型的A型花岗岩类

表2 姚村岩体全岩主量元素（%）、稀土元素和微量元素含量（10⁻⁶）

Table 2 The content of main elements (%), rare earth elements and trace elements(10⁻⁶) of the Yaocun pluton

| 样品号	16YC-1	16YC-2	16YC-3	16YC-5	16YC-6	16YC-7	16YC-8	16YC-9	16YC-10	8852-1-3	8853-1-1	8849-1-1
岩性	细粒正长花岗岩			细粒似斑状正长花岗岩					中粗粒正长花岗岩			
SiO_2	76.48	76.53	76.18	75.58	76.12	76.51	76.59	75.46	76.48	77.55	76.98	77.39
Al_2O_3	12.33	12.38	12.62	12.73	12.61	12.22	12.26	12.68	12.83	11.85	12.31	12.17
Fe_2O_3	0.72	0.82	0.83	0.68	0.49	0.58	0.57	0.59	0.8	0.68	0.69	0.54
FeO	0.16	0.35	0.38	0.52	0.48	0.36	0.42	0.94	0.1	0.23	0.14	0.28
CaO	0.65	0.48	0.23	0.62	0.59	0.57	0.61	0.58	0.58	0.34	0.45	0.28
MgO	0.14	0.13	0.14	0.18	0.18	0.14	0.14	0.29	0.13	0.07	0.1	0.13
Na_2O	3.51	3.45	3.48	3.52	3.65	3.73	3.48	3.28	3.52	3.26	3.54	3.08
K_2O	4.80	4.83	4.81	4.93	4.86	4.75	4.63	4.91	5.23	5.1	4.9	5.38
TiO_2	0.11	0.09	0.12	0.16	0.14	0.11	0.14	0.22	0.13	0.08	0.13	0.14
MnO	0.02	0.02	0.05	0.06	0.05	0.07	0.07	0.05	0.06	0.03	0.06	0.04
P_2O_5	0.01	0.02	0.01	0.04	0.02	0.01	0.02	0.02	0.02	0.01	0.01	0.02
烧失量	1.06	0.90	0.88	0.64	0.53	0.68	0.66	0.62	0.64	0.59	0.57	0.43
总量	99.99	100.00	99.73	99.66	99.72	99.73	99.59	99.64	100.42	99.79	99.88	99.88
A/CNK	1.01	1.05	1.11	1.04	1.02	0.99	1.04	1.08	1.03	1.03	1.03	1.07
A/NK	1.12	1.14	1.15	1.14	1.12	1.08	1.14	1.18	1.12	1.09	1.11	1.12
La	34.40	35.60	44.20	52.60	58.02	47.73	65.27	61.19	43.40	35.50	47.20	44.50
Ce	52.40	56.59	60.84	90.48	92.55	75.62	98.91	104.91	73.50	62.20	84.20	75.50
Pr	5.69	4.86	4.69	9.24	9.33	6.92	8.67	10.72	6.77	5.21	7.93	6.97
Nd	17.17	13.96	15.59	30.15	27.02	19.62	24.88	34.99	22.30	15.30	26.40	23.10
Sm	3.05	2.98	3.28	5.38	4.16	2.95	3.85	6.24	3.06	2.57	3.75	3.20
Eu	0.28	0.23	0.25	0.66	0.43	0.27	0.35	0.65	0.39	0.28	0.40	0.36
Gd	3.17	2.36	3.73	4.54	4.57	3.56	4.67	5.51	2.24	2.77	2.86	2.27
Tb	0.47	0.38	0.79	0.82	0.59	0.47	0.62	0.97	0.37	0.42	0.43	0.38
Dy	2.73	2.36	5.41	4.56	3.22	2.68	3.49	5.38	2.61	2.98	2.96	2.65
Ho	0.59	0.54	1.26	0.98	0.72	0.63	0.79	1.14	0.56	0.63	0.63	0.57
Er	1.88	1.92	4.10	3.12	2.41	2.21	2.66	3.46	1.88	1.86	2.13	1.95
Tm	0.39	0.36	0.64	0.60	0.51	0.50	0.57	0.65	0.36	0.42	0.41	0.39
Yb	2.78	2.84	4.95	4.25	3.85	3.98	4.36	4.33	2.91	2.80	3.35	3.13
Lu	0.43	0.46	0.75	0.64	0.64	0.67	0.71	0.63	0.48	0.54	0.56	0.53
Li	28.30	27.50	23.20	38.20	42.60	52.90	31.80	48.00	33.70	39.20	24.40	70.80
Be	6.39	5.77	6.54	32.10	9.86	4.43	7.03	6.00	25.10	8.75	9.48	8.60
Rb	214	291	320	341	354	229	266	310	368	440	323	398
Sr	35.6	64.0	20.0	49.6	29.1	66.0	72.8	52.0	34.8	12.1	32.4	20.4
Nb	17.7	27.6	28.5	30.3	32.9	24.4	25.2	26.3	31.5	18.2	31.7	37.9
Mo	0.71	1.13	2.56	7.57	3.13	0.74	5.83	1.69	2.84	1.60	2.45	1.25
Ni	0.66	0.28	0.24	0.20	0.30	1.42	0.34	0.59	0.06	0.14	0.06	0.05
Ba	134	261	66	100	98	151	164	196	103	139	117	98
Y	16.40	21.60	26.10	19.44	14.63	21.95	26.87	22.80	17.70	9.54	20.00	17.70
Ta	1.55	2.16	2.74	2.20	2.35	1.85	2.18	1.82	2.06	1.31	2.05	2.52
Pb	24.60	22.40	28.30	21.80	26.50	26.20	24.20	23.60	20.40	23.90	20.90	19.40
Th	21.20	23.10	23.10	24.70	30.40	14.30	30.50	20.70	26.50	29.30	30.40	27.50
U	6.87	5.56	10.60	7.63	10.10	3.85	9.48	4.75	7.81	7.40	6.78	5.40
Sc	2.14	4.53	3.10	3.72	2.76	3.67	4.42	3.84	4.09	3.26	3.99	5.02
Cr	8.83	6.91	10.30	6.50	6.29	9.24	14.60	14.20	0.28	0.26	0.27	1.99
Co	1.36	3.29	0.40	0.77	0.49	5.52	1.59	2.63	0.27	0.39	0.15	0.13
Ga	15.20	18.60	18.70	18.40	19.40	18.70	16.40	19.10	18.30	19.10	17.80	17.90
Zr	106	207	127	145	161	122	175	299	124	92.3	132	140
Hf	3.73	7.93	6.79	4.94	5.74	8.33	5.61	7.93	5.55	4.75	6.13	6.77
Sn	3.20	4.20	4.50	2.50	2.70	2.90	4.20	2.90	3.42	3.75	2.72	4.34
Zn	19.20	42.10	13.70	21.00	15.80	61.90	31.20	43.50	12.10	11.10	11.10	9.87
$\sum REE$	125	125	150	208	208	168	220	241	161	133	183	166
Eu/Eu*	0.28	0.27	0.22	0.41	0.30	0.25	0.25	0.34	0.46	0.32	0.37	0.41
(La/Yb)$_N$	8.88	8.99	6.40	8.88	10.81	8.60	10.74	10.14	10.70	9.09	10.11	10.20
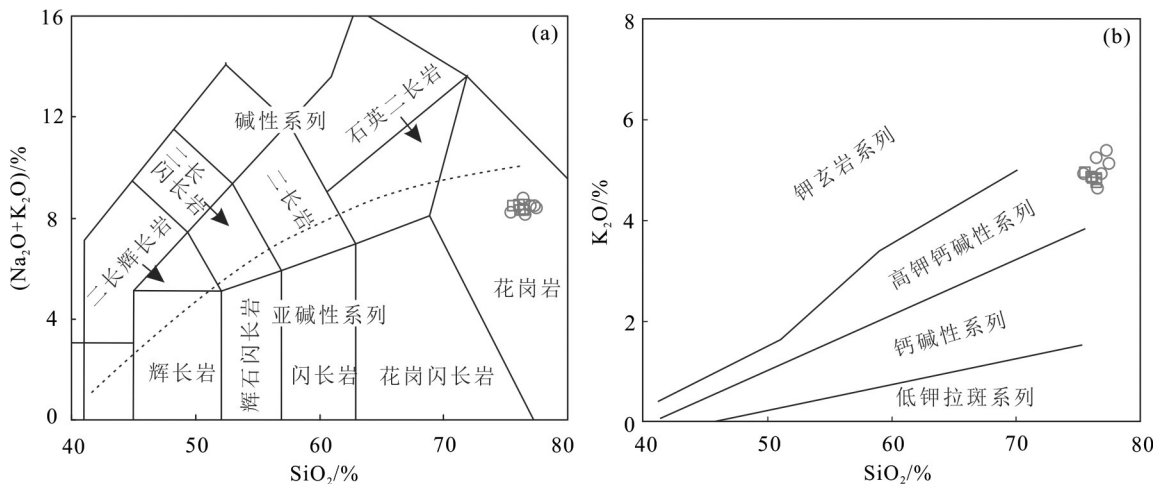
图4 姚村岩体TAS分类图解(a)(据Middlemost, 1994)和K₂O−SiO₂图解(b)(据Peccerillo et al., 1976)(圆形为中粗粒正长花岗岩,正方形为细粒似斑状正长花岗岩)

Fig.4 Alkali vs. silica (TAS) diagram (a, after Middlemost, 1994) and SiO₂ − K₂O diagram(b, after Peccerillo et al., 1976) of the Yaocun pluton

(The circle represents medium− to coarse−grained syenogranite, and the square represents fine−grained porphyritic syenogranite.)

似(Loiselle & Wones, 1979; Whalen et al., 1987; Bonin, 2007; Frost & Frost, 2008)。在前人提出的花岗岩类型判别图解中(图6),包括 Na₂O−K₂O 图解(图6a,据 Collins et al., 1982)、FeO^T/(FeO^T+MgO)−SiO₂ 图解(图6b,据 Frost & Frost, 2011)、(Na₂O+K₂O)/CaO−1000×Ga/Al 和 Nb−1000×Ga/Al 图解(图6c 和图6d,据 Whalen et al., 1987),除个别样品点外,姚村岩体基本落入A型花岗岩范围内。

另外,根据 Watson and Harrison(2005)提出的锆饱和温度计,计算得到的姚村岩体成岩温度为785～899℃(平均827℃),指示姚村岩体形成温度

较高,与典型A型花岗岩类似,而明显高于一般的I型和S型花岗岩的锆石饱和温度(<800℃)。因此,姚村岩体为A型花岗岩。

5.3 岩石成因及源区性质

尽管A型花岗岩一般认为形成于伸展的构造环境,但是对其成因过程还存在不同认识,主要有两种模式:(1)幔源玄武质岩浆的结晶分异,并伴随或不伴随地壳混染(Loiselle & Wones, 1979; Turner et al., 1992; Mushkin et al., 2003; Bonin, 2007);(2)特殊地壳原岩的部分熔融(Collins et al., 1982; Whalen et al., 1987; Creaser et al., 1991)。
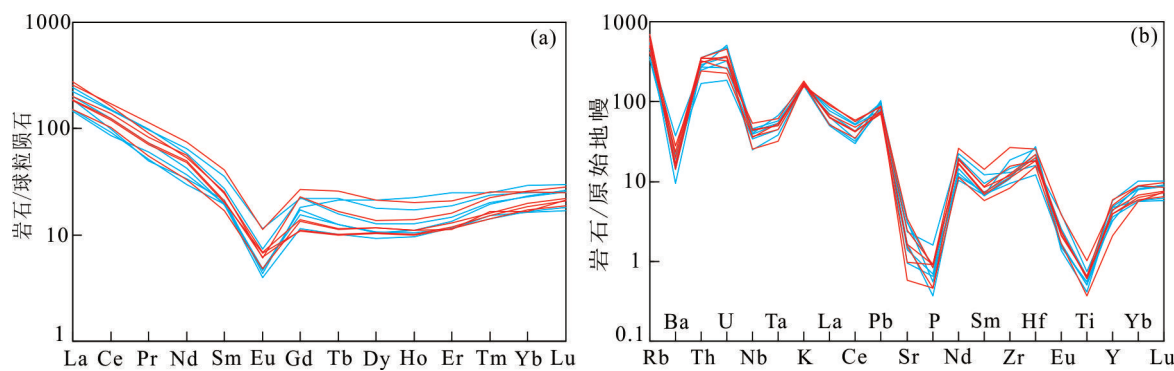

图5 姚村岩体球粒陨石标准化稀土元素配分图(a)和原始地幔标准化微量元素蛛网图(b)

(球粒陨石和原始地幔的标准值据 Sun and McDonough, 1989)(红线为中粗粒正长花岗岩,蓝线为细粒似斑状正长花岗岩)

Fig.5 Chondrite−normalized REE distribution diagram of Yaocun pluton (a) and primitive mantle−normalized trace element spider (b)

Chondrite−normalized rare earth element (a) and primitive−mantle−normalized trace element date(b) for samples of the Yaocun pluton.

(Normalizing values are from Sun & McDonough 1989). (The red line represents medium− to coarse−grained syenogranite, and the blue line represents fine−grained porphyritic syenogranite.)

表3 姚村岩体全岩Sr−Nd同位素测试结果
Table 3　Sr−Nd isotope compositions of representative samples from the Yaocun pluton

样品号	Rb/10⁻⁶	Sr/10⁻⁶	⁸⁷Rb/⁸⁶Sr	⁸⁷Sr/⁸⁶Sr	±2σ	⁸⁷Sr/⁸⁶Sr(I)	Sm/10⁻⁶	Nd/10⁻⁶	¹⁴⁷Sm/¹⁴⁴Nd	¹⁴³Nd/¹⁴⁴Nd	2σ	ε_Nd(t)	TDM2
H8852-1-3	440	12.1	105.5	0.900426	0.000016	0.7101	1.57	15.3	0.061979	0.512207	0.000005	-6.23	1534
H8853-1-1	323	32.4	28.9	0.761957	0.000015	0.7098	3.75	26.4	0.085795	0.512253	0.000011	-5.71	1494

注：t=127 Ma。

通常由幔源玄武质岩浆结晶分异而成的A型花岗岩一般会和大规模基性岩共生（Turner et al., 1992），并具有亏损的同位素组成（Kemp and Hawkesworth, 2005）。宣城地区暂未发现与第三阶段岩浆作用同时期的基性岩浆岩。同时，姚村岩体$\varepsilon_{Nd}(t)$值变化于−6.2~−5.7，$\varepsilon_{Hf}(t)$值介于−13.9~−5，具有较为富集的同位素组成，据此推断，姚村岩体不是由幔源玄武质岩浆结晶分异而来，其主体上应为壳源岩浆岩。

$(La/Sm)_N$对La以及Zr/Nb对Zr的正相关表明部分熔融可能是控制姚村岩体成因的主要岩浆过程（图7）。在花岗岩源岩判别图解中，姚村岩体投影

于变泥质和变杂砂岩的部分熔融产生的熔体区域内（图8a），并且排除镁铁质组分的混入（图8b），表明姚村岩体地球化学特征继承其原岩。

下扬子陆块具有"一盖两底"的格局，新太古代—新元古代崆岭群—董岭岩群为"江北型"基底，中新元古代双桥山群—溪口岩群（上溪群）为"江南型"基底（常印佛和董树文等，1996）。姚村正长花岗岩相比于崆岭群灰色片麻岩（Xing et al., 1994；凌文黎等，1998；Ma et al., 2000）及董岭岩群角闪岩（Xing et al., 1994）具有相对较高的Nd同位素。同时锆石Hf同位素显示，崆岭群TTG片麻岩和董岭岩群中锆石Hf同位素组成远比姚村正长花岗岩的

表4 姚村岩体（8849−1−1）锆石Hf同位素组成
Table 4　Hf isotopic compositions of zircon grains from the Yaocun pluton determined by LA−MC−ICP−MS

| 测点号	年龄/Ma	¹⁷⁶Yb/¹⁷⁷Hf	¹⁷⁶Lu/¹⁷⁷Hf	¹⁷⁶Hf/¹⁷⁷Hf	1σ	¹⁷⁶Hf/¹⁷⁷Hf_i	ε_Hf(t)	1σ	T_DM1/Ma	T_DM2/Ma	f_Lu/Hf
8849-1-1-1	131	0.028145	0.001041	0.282416	0.000017	0.282413	-9.8	0.58	1184	1808	-0.97
8849-1-1-3	131	0.046703	0.001636	0.282303	0.000023	0.282299	-13.9	0.79	1364	2062	-0.95
8849-1-1-4	131	0.032340	0.001152	0.282499	0.000011	0.282497	-6.9	0.40	1070	1624	-0.97
8849-1-1-5	131	0.036898	0.001329	0.282542	0.000010	0.282539	-5.4	0.33	1014	1529	-0.96
8849-1-1-6	131	0.040087	0.001416	0.282521	0.000012	0.282518	-6.1	0.43	1046	1576	-0.96
8849-1-1-7	131	0.037099	0.001316	0.282457	0.000012	0.282453	-8.4	0.44	1135	1719	-0.96
8849-1-1-8	131	0.028963	0.001074	0.282410	0.000014	0.282407	-10.0	0.49	1194	1823	-0.97
8849-1-1-9	131	0.032431	0.001153	0.282464	0.000015	0.282462	-8.1	0.52	1119	1701	-0.97
8849-1-1-10	131	0.038485	0.001401	0.282322	0.000020	0.282319	-13.2	0.69	1328	2018	-0.96
8849-1-1-11	131	0.035839	0.001363	0.282493	0.000021	0.282490	-7.1	0.73	1085	1639	-0.96
8849-1-1-12	131	0.048463	0.001728	0.282428	0.000021	0.282424	-9.4	0.74	1188	1785	-0.95
8849-1-1-13	131	0.025480	0.000949	0.282506	0.000012	0.282504	-6.6	0.42	1054	1607	-0.97
8849-1-1-14	131	0.055412	0.001992	0.282539	0.000010	0.282534	-5.5	0.35	1037	1540	-0.94
8849-1-1-15	131	0.030669	0.001122	0.282453	0.000013	0.282450	-8.5	0.44	1134	1726	-0.97
8849-1-1-16	131	0.047731	0.001770	0.282498	0.000014	0.282493	-7.0	0.48	1090	1631	-0.95
8849-1-1-17	131	0.043412	0.001551	0.282426	0.000009	0.282422	-9.5	0.31	1185	1788	-0.95
8849-1-1-18	131	0.051944	0.001838	0.282470	0.000014	0.282466	-8.0	0.48	1132	1693	-0.94
8849-1-1-19	131	0.042900	0.001603	0.282504	0.000020	0.282500	-6.7	0.69	1076	1616	-0.95
8849-1-1-20	131	0.036066	0.001290	0.282422	0.000010	0.282418	-9.6	0.35	1184	1798	-0.96
8849-1-1-21	131	0.037033	0.001340	0.282526	0.000011	0.282523	-5.9	0.39	1037	1565	-0.96
8849-1-1-22	131	0.028470	0.001049	0.282417	0.000013	0.282414	-9.8	0.45	1183	1807	-0.97
8849-1-1-23	131	0.037579	0.001413	0.282495	0.000015	0.282492	-7.0	0.51	1083	1635	-0.96
8849-1-1-24	131	0.039977	0.001438	0.282552	0.000014	0.282548	-5.0	0.49	1004	1508	-0.96
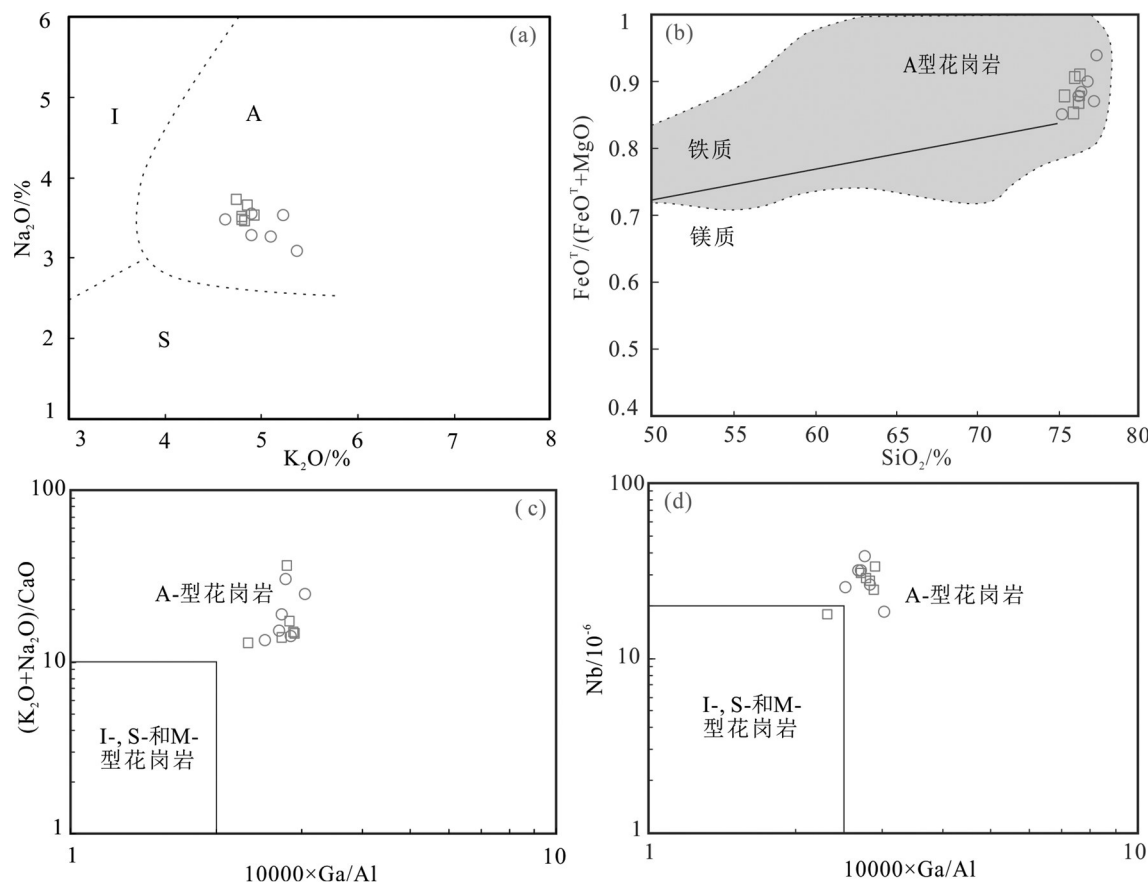
图6 姚村A型花岗岩判别图解（底图a据Collins et al., 1982；底图b据Frost and Frost, 2011; 底图c和d据Whalen et al., 1987）
（图例同图4）
Fig.6 Chemical discrimination diagrams of the Yaocun A−type granitic pluton: (a) Na₂O vs. K₂O; (b) FeOᵀ/(FeOᵀ+MgO) vs.SiO₂; (c)
(K₂O+ Na₂O) /CaO vs. 10, 000 Ga; (d) Nb vs. 10, 000 Ga
(a after Collins et al., 1982; b after Frost and Frost, 2011; c and d after Whalen et al., 1987). Symbols are the same as in Fig. 4
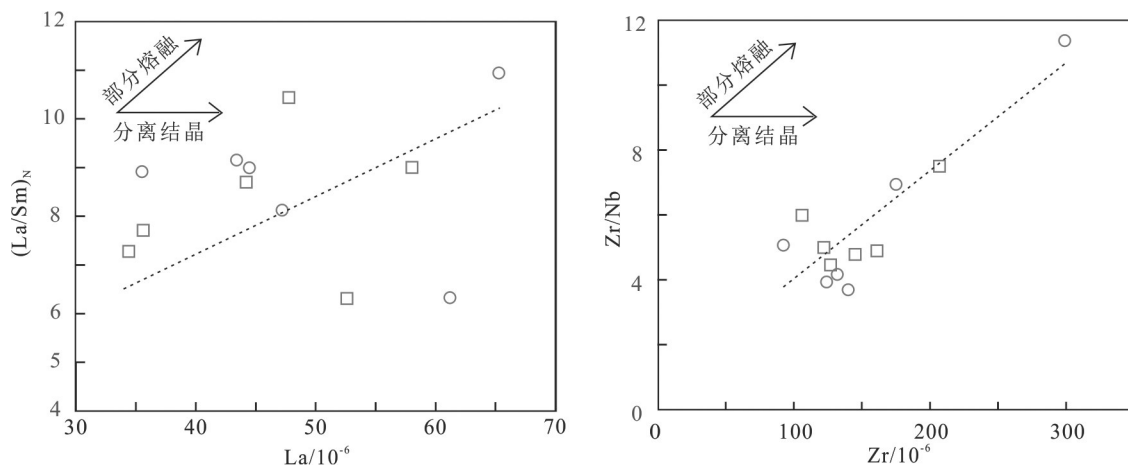

图7 姚村岩体岩浆过程判别图解 (a)La−La/Sm图解; (b) Zr−Zr/Nb 图解（图例同图4）
Fig.7 (a) La vs. (La/Sm) ₙ ; (b) Zr vs. Zr/Nb discrimination diagram of the Yaocun A−type granitic pluton
(Symbols are the same as Fig. 4)
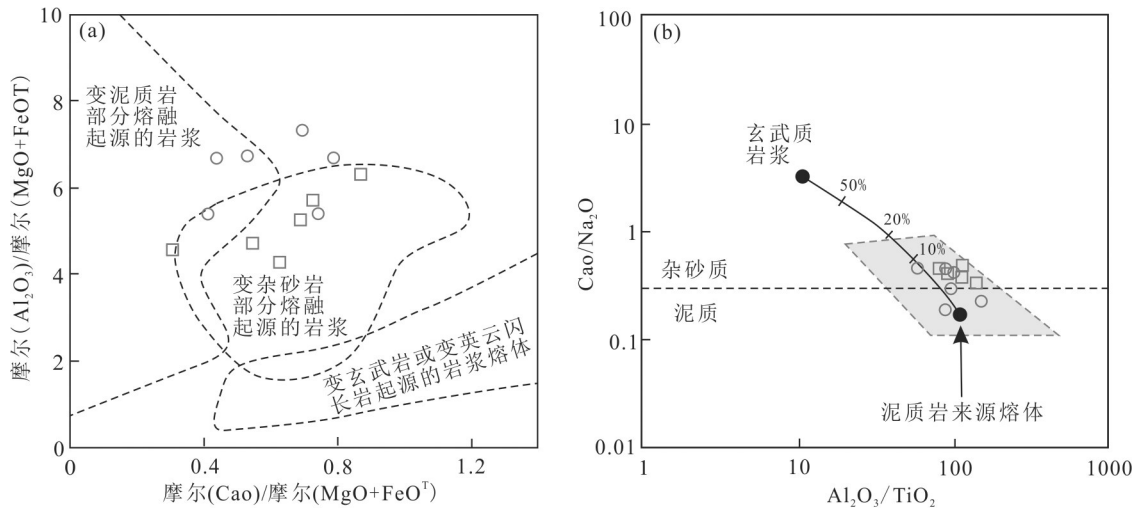
图 8 姚村岩体源岩判别图解：(a)摩尔 Al₂O₃/(MgO+FeOᵀ)−摩尔 CaO/(MgO+FeOᵀ)图解（据 Altherr et al., 2000）; (b)Al₂O₃/TiO₂−CaO/Na₂O 图解（据 Sylvester., 1998）（图例同图 4）

Fig.8 (a) Molar Al₂O₃/(MgO + FeOᵀ) vs. CaO/(MgO + FeOT) and (b) Al₂O₃/TiO₂ vs. CaO/Na₂O diagrams of the Yaocun A−type granitic pluton (a after Altherr et al., 2000 and b after Sylvester., 1998). Symbols are the same as in Fig. 4

锆石 Hf 同位素要富集（Zhang et al., 2006；Guo et al., 2014；Zhang et al., 2015；Chen et al., 2016），表明以崆岭群和董岭岩群所代表的古老地壳不是岩浆源区。

姚村岩体样品的 Nd 模式年龄（T_{DM2}=1493~1532 Ma）及锆石 Hf 模式年龄（T_{DM2}=1508~2062 Ma）表明原岩为中元古代时期物质。在 t−εHf(t)图解中，姚村正长花岗岩的 εNd(t)值落于双桥山群和溪口岩群的 Nd 同位素演化线范围内（图 9a），同样在 t−εHf(t)图解中，由中元古代地壳部分熔融而成的新元古代花岗岩的 Hf 同位素演化线范围全部覆盖姚村岩体的 εNd(t)值（图 9b）。以上同位素特征表明姚村岩体为这些中元

古代地壳物质在约 127 Ma 时期重熔的产物。

5.4 构造环境

对于华南东部燕山期构造背景，曾存在逆冲推覆成因（Hsü et al., 1988）、岩石圈伸展与软流圈地幔上涌（Li, 2000; Wang et al., 2003）、中生代开始的整个中国东海岸裂谷（Gilder et al., 1991）以及华南中生代地幔柱上升（Deng et al., 2004）等多种不同认识，但目前绝大多数学者已认可古太平洋板块对欧亚板块的俯冲消减作用才是形成华南东南部燕山期花岗质岩石−火山岩的根本动力学机制（Zhou & Li, 2000；Zhou et al., 2006；Li & Li , 2007；Sun et al.,
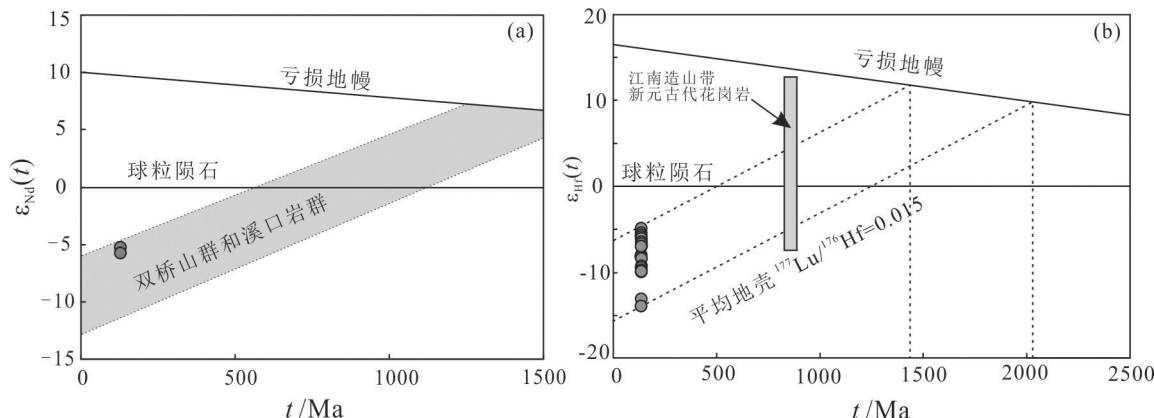

图 9 姚村岩体全岩 εNd(t)−t 图解（a,双桥山群和溪口岩群全岩 Nd 同位素据 Chen & Jahn, 1998）和锆石 εHf(t)−t 图解（b,新元古代花岗岩锆石 Hf 同位素据 Zhang & Zheng, 2013; Wang et al., 2013）

Fig.9 εNd(t) vs. t diagram (a, after Chen & Jahn, 1998) and εHf(t) vs. t diagram (b, after Zhang & Zheng, 2013; Wang et al., 2013) of the Yaocun pluton

2007; Chen et al., 2008; Wang et al., 2011; He & Xu，2012; Li et al., 2012; 吕庆田等,2019)。

虽然俯冲作用的精细过程还存在多种观点,但对于华南东部(140~125 Ma)的岩浆活动,一般认为形成于伸展的构造环境(Li, 2000; Wang et al, 2003; Zhou et al., 2013; 邢光福等, 2017),皖南江南造山带晚期阶段136~122 Ma的岩浆活动也受控于此构造背景之下(闫峻等,2017)。

姚村A型花岗岩的侵位时代在127 Ma左右,邻区其他A型花岗岩,如刘村岩体(132 Ma,陈芳等,2014)、九华山岩体(130~131 Ma, Wu et al., 2012)、黄山岩体(125~127 Ma,薛怀民等,2009)、伏岭岩体(124 Ma, Zhou et al., 2013)、牯牛降岩体(130 Ma,谢建成等, 2012)、铜山岩体(129 Ma, Jiang et al., 2011)、杨梅湾岩体(135 Ma, Yang et al., 2012)、白菊花尖岩体(126 Ma, Wong et al., 2009)、大茅山(126~122 Ma, Jiang et al., 2011)、三清山(132~130 Ma, Sun et al., 2015)、灵山岩体(134~132 Ma, Wang et al., 2018)等,年龄均集中在135~124 Ma。

广泛出露的A型花岗岩充分说明此时本区处于弧后的伸展环境(薛怀民等,2009;张舒等,2009;Wu et al., 2012; Zhou et al., 2013; 陈芳等, 2014;高冉等,2017)。从侏罗纪到白垩纪,随着板片俯冲角度增加,弧后延伸作用逐渐增强(Zhou et al., 2006)。后续的软流圈上涌导致了陆下岩石圈地慢的熔融,产生了大量的玄武质岩浆底侵至下地壳(Zhou & Li, 2000)。玄武质岩浆的底侵为中元古代基底沉积岩的大范围部分熔融提供了热源,从而产生了A型花岗质岩浆。

6 结 论

(1)姚村岩体形成年龄为(127.6 ±1.4)Ma,属早白垩世岩浆作用的产物,对应于皖南江南造山带第二阶段岩浆活动。

(2)姚村岩体具有较高的(Na₂O+K₂O)含量、FeOᵀ/(FeOᵀ+MgO)比值、高场强元素和稀土元素含量,同时具有较低的Ba、Sr、Ti和Eu含量以及较高的锆石饱和温度,表明姚村岩体为A型花岗岩。

(3)全岩Sr-Nd同位素和锆石Hf同位素特征指示姚村岩体为下扬子中元古代地壳物质部分熔融的产物,形成于早白垩世古太平洋板块俯冲作用之

后弧后拉伸环境下。

References

Altherr R, Holl A, Hegner E, Langer C, Kreuzer H. 2000. High–potassium, calcalkaline I– type plutonism in the European Variscides,northern Vosges (France) and northern Schwarzwald (Germany) [J]. Lithos, 50: 51–73.

Blichert–Toft J, Albarede F. 1997. The Lu–Hf isotope geochemistry of chondrites and the evolution of the mantle–crust system[J]. Earth and Planet Science Letter, 148(1/2): 243–258.

Bonin B. 2007. A–type granites and related rocks: Evolution of a concept, problems and prospects[J]. Lithos, 97, 1–29.

Chang Yinfo, Dong Shuwen. 1996. On tectonics of "poly– basement withone cover" in middle– lower Yangtze craton China[J]. Volcanology and Mineral Resources, 17(1/2): 1– 15 (in Chinese with English abstract).

Chen C H, Lee C Y, Shinjo R. 2008. Was there Jurassic paleo–Pacific subduction in South China? Constraints from ⁴⁰Ar/³⁹Ar dating, elemental and Sr–Nd–Pb isotopic geochemistry of the Mesozoic basalts[J]. Lithos, 106(1–2): 83–92.

Chen Fang, Wang Denghong, Du Jianguo, Xu Wei, Hu Haifeng, Wang Keyou, Yu Youlin, Tang Jinlai. 2014. Geochemical characteristics and LA– ICP– MS zircon U– Pb geochronology of the Liucun monzogranite in ningguo, Anhui Provinceand and their geological significance[J]. Acta Geologica Sinica, 88(5): 869–882 (in Chinese with English abstract).

Chen Jun, Wang Hui, Wang Lijuan, Guan Junpeng. 2018. Petrogenesis of Jinniu rock mass in Chuzhou area：Melting of delaminated lower crust or mixing of crust and mantle[J]. Geology in China, 45(1): 110–128(in Chinese with English abstract).

Chen Z H, Xing G F. 2016. Geochemical and zircon U–Pb–Hf–O isotopic evidence for a coherent Paleoproterozoic basement beneath the Yangtze Block, South China[J]. Precambrian Research, 279:81–90.

Collins W J, Beams S D, White A J R,Chappell B W. 1982. Nature and origin of A–type granites with particular reference to southeastern Australia[J]. Contributions to Mineralogy and Petrology, 80, 189–200.

Creaser R A, Price R C, Wormald R J. 1991. A–type granites revisited: Assessment of residual source model[J]. Geology, 19:163–166.

Deng J F, Mo X X, Zhao H L, Wu Z X, Luo Z H, Su S G. 2004. A newmodel for the dynamic evolution of Chinese lithosphere: 'continental roots– plume tectonics' [J]. Earth– Science Reviews, 65 (3/4): 223–275.

Frost B R, Frost C D. 2008. A geochemical classification for feldspathic igneous rocks[J]. Journal of Petrology, 49:1955–1969.

Frost C D, Frost B R. 2011. On ferroan (A–type) granitoids: their compositional variability and modes of origin[J]. Journal of Petrology 52, 39–53.

Gao Ran, Yan Jun, Li Quanzhong, Liu Xiaoqiang, Wang Sinuo. 2017. Petrogenesis of Tanshan Pluton in the Southern Anhui Province: Chronological and geochemical constraints[J]. Geological Journal of China Universities, 23(2): 227−243 (in Chinese with English abstract).

Gilder S A, Keller G R, Luo M, Goodell P C. 1991. Eastern Asia and the Western Pacific timing and spatial distribution of rifting in China[J]. Tectonophysics, 197(2−4): 225−243.

Griffin W L, Wang X, Jackson S E, et al. 2002. Zircon geochemistry and magma mixing, SE China: In− situ analysis of Hf isotopes, Tonglu and Pingtan igneous conplexes[J]. Lithos, 61: 237−269.

Guan Junpeng, Weii Fubiao, Sun Guoxi, Huang Jianping, Wang Lijuan. 2015. Zircon U−Pb dating of intermediate− acid intrusive rocks in the middle section of Ningzhen district and their metallogenic implications[J]. Geotectonica et Metallogenia, 39(2): 344−354 (in Chinese with English abstract).

Guo J L, Gao S, Wu Y S. 2014. 3.45 Ga granitic gneisses from the Yangtze Craton, South China: Implications for Early Archean crustal growth[J]. Precambrian Resiearch, 242, 82−95.

Chen J F, Jahn B M. 1998. Crust evolution of southestem China: Nd and Sr isotopic evidence[J]. Tectonophysics, 284(1/2): 101−133.

He Z Y, Xu X S. 2012. Petrogenesis of the Late Yanshanian mantle− derived intrusions in southeastern China: Response to the geodynamics of paleo− Pacific plate subduction[J]. Chemical Geology, 328: 208−221.

Hou Kejun, Li Yanhe, Tian Yourong. 2009. In situ U−Pb zircon dating using laser ablation− multi ion counting− ICP− MS[J]. Mineral Deposits, 28(4): 481−492 (in Chinese with English abstract).

Hsü K J, Sun S, Li J L, Chen H H, Pen H P, Sengor A M C. 1988. Mesozoic overthrust tectonics in south China[J]. Geology, 16(5): 418−421.

Jiang Y H, Zhao P, Zhou Q, Liao S Y, Jin G D. 2011. Petrogenesis and tectonic implications of Early Cretaceous SandA−type granites in the northwest of the Gan−Hang rift, SE China[J]. Lithos, 121, 55−73.

Kemp A I S, Hawkesworth C J. 2005. Granitic perspectives on the generation and secular evolution of the continental crust[C]// Rudnick R J (ed.). Treatise on Geochemistry. Pergamon, Oxford, 1−64.

Li X H. 2000. Cretaceous magmatism and lithospheric extension in southeast China[J]. Journal of Asian Earth Sciences, 18 (3): 293−305.

Li Z X, Li X H. 2007. Formation of the 1300 km wide intracontinental orogen and postorogenic magmatic province in Mesozoic South China: A flat slab subduction model[J]. Geology, 35(2): 179−182.

Li Z X, Li X H, Chung S L, Lo C H, Xu X S and Li W X. 2012. Magmatic switch on and switch off along the South China continental margin since the Permian: Transition from an Andean type to a Western Pacific type plate boundary[J]. Tectonophysics, 532/535: 271−290.

Ling Wenli, Gao Shan, Zheng Haifei, Zhou Lian, Zhao Zubin. 1998. An Sm− Nd isotopic dating study of the Archean Kongling

complex in the Huangling area of the Yangtze craton[J]. Chinese Science Bulletin (Chinese Version), 43(1): 86−89 (in Chinese).

Liu Y S, Gao S, Hu Z C, Wang D B. 2010. Continental and oceanic crust recycling−induced melt−peridotite interactions in the Trans− North China Orogen: U−Pb dating, Hf isotopes and trace elements in zircons of mantle xenoliths[J]. Journal of Petrology, 51: 537−571.

Liu Y S, Hu ZC, Gao S, Chen H L. 2008. In situ analysis of major and trace elements of anhydrous minerals by LA− ICP− MS without applying an internal standard[J]. Chemical Geology, 257: 34−43.

Loiselle M C, Wones D R. 1979. Characteristics of anorogenic granites[J]. Geological Society of America Abstracts with Programs, 11(7): 468.

Ludwig K R. 2003. Isoplot/EX Version 2.49: A Geochronological Toolkit for Microsoft Excel[M]. Berkeley: Berkeley Geochronology Center Special Publication, 1a: 1−56.

Lü Qingtian, Meng Guixiang, Yan Jiayong, Zhang Kun, Zhao Jinhua, Gong Xuejing. 2019. Multi−scale exploration of mineral system: Concept and progress—A case study in the middle and lower reaches of the Yangtze River Metallogenic Belt[J]. Geology in China, 46(4): 673−689(in Chinese with English abstract).

Ma C, Ehlers C, Xu C, et al. 2000. The roots of Ac Dabieshan ultrahigh− pressure metamorphic terrane: constraints from geochemistry and Nd− Sr isotope systematics[J]. Precambrian Research, 102: 279−301.

Mao Jingwen, Holly S, Du Andao, Zhou Taofa, Mei Yanxiong, Li Yongfeng, Zang Wenshuan, Li Jinwen. 2004. Molybdenite Re−Os precise dating for molybdenite from Cu− Au− Mo deposits in the Middle−Lower Reaches of Yangtze River Belt and its implications for mineralizatotn[J]. Acta Geologica Sinica, 78(1): 121− 131 (in Chinese with English abstract).

Middlemost, E A K. 1994. Naming materials in the magma/igneous rock system[J]. Earth Science Reviews, 37: 215−224.

Mushkin A, Navon O, Halicz L, Hartmann G and Stein M. 2003.The petrogenesis of A− type magmas from the Amram Massif, southernIsrael[J]. Journal of Petrology, 44(5): 815−832.

Peccerillo A, Taylor S R.1976. Geochemistry of eocene calc−alkaline volcanic rocks from the Kastamonu Area, Northern Turkey[J]. Contributions to Mineralogy and Petrology, 58: 63−81.

Scherer E, Munker C and Mezger K. 2001. Calibration of the lutetium− hafnium clock[J]. Science, 293: 683−687.

Sun F J, Xu X S, Zou H B, Xia Y. 2015. Petrogenesis and magmatic evolution of ~130 Ma A− type granites in Southeast China[J]. Journal of Asian Earth Sciences 98, 209−224.

Sun S S, McDonough W F. 1989. Chemical and isotopic systematics of oceanic basalt: implications for mantle composition and processes[C]//Sanders A D, Norry M J (ed.). Magmatism in the Ocean Basins. Geological Society, London, Special Publications, 42: 313−345.

Sun W D, Ding X, Hu Y H, Li X H. 2007. The golden transformation of the Cretaceous plate subduction in the west Pacific[J]. Earth and

Planetary Science Letters, 262(3−4): 533−542.

Sylvester P J. 1998. Post− collisional strongly peraluminous granites[J]. Lithos, 45(1−4): 29−44.

Xing F M, Xu X, Li Z C, 1994. Discovery of the Early Proterozoic basement in the Middle−Lower

Reaches of Yangtze River and its significance[J]. Chinese Science Bulletin, 2: 135−139.

Turner S P, Foden J D, Morrison R S. 1992. Derivation of some Atype magmas by fractionation of basaltic magma: An example from the Padthaway Ridge, South Australia[J]. Lithos, 28, 151−179.

Vervoort J D, Blichert−Toft J. 1999. Evolution of the depleted mantle: Hf isotope evidence from juvenile rocks through time [J]. Geochimica et Cosmochimica Acta, 63(3/4): 533−556.

Wang Cunzhi, Huang Zhizhong, Zhao Xilin, Chu Pingli, Huang Wencheng, Song Shiming, Chen Zhihong. 2018. Geochronology, geochemistry and petrogenesis of Early Cretaceous acid volcanic rocks at Shuidong Area, Xuancheng City in the Middle− Lower Yangtze River Belt[J]. Acta Petrologica et Mineralogica, 37(5): 697−715 (in Chinese with English abstract).

Wang C Z, Zhao X L, Huang Z Z, Xing G F, Wang L X. 2018. Early Cretaceous Extensional tectonism related petrology of the Gan Hang Belt SE China: Lingshan A type granite at ca. 130 Ma[J]. Geological Journal, 53(6): 2487−2506.

Wang F Y, Ling M X, Ding X, Hu Y H, Zhou J B, Yang X Y, Liang H Y, Fan W M, Sun W D. 2011. Mesozoic large magmatic events and mineralization in SE China: Oblique subduction of the Pacific plate[J]. International Geology Review, 53(5−6): 704−726.

Wang Jiqiang, Sun Weian, Yuan Feng, Shang Shigui, Zhou Taofa, Zhong Fuming, Zhang Ruofei. 2017. Geological characteristics, rock−forming epoch and genesis of the Danizhuang Cu deposit in Luzong basin[J]. Geology in China, 44(1): 86−100(in Chinese with English abstract).

Wang X L, Zhou J C, Wan Y S, Kitajima K, Wang D, Bonamici C, Qiu J S, Sun T. 2013. Magmatic evolution and crustal recycling for Neoproterozoic strongly peraluminous granitoids from southern China: Hf and O isotopes in zircon[J]. Earth and Planetary Science Letters, 366 (2): 71−82.

Wang Y J, Fan W M, Guo F, Peng T P, Li C W. 2003. Geochemistry of Mesozoic mafic rocks adjacent to the Chenzhou Linwu fault, South China:Implications for the lithospheric boundary between the Yangtze and Cathaysia blocks[J]. International Geology Review, 45 (3): 263−286.

Watson E B, Harrison T M. 2005. Zircon thermometer reveals minimum melting conditions on earliest Earth[J]. Science, 308 (5723): 841−844.

Whalen J B, Currie K L, Chappell B W. 1987. A− type granites: Geochemical characteristics, discrimination and petrogenesis[J]. Contributions to Mineralogy and Petrology, 95: 407−419.

Wong J, Sun M, Xing G F, Li X H, Zhao G C, Wong K, Yuan C, Xia X P, Li L M. & Wu FY. 2009. Geochemical and zircon U−Pb and Hf isotopic study of the Baijuhuajian metaluminous A− type granite: extension at 125−100 Ma and its tectonic significance for South China[J]. Lithos, 112: 289−305.

Wu F Y, Ji W Q, Sun D H. 2012. Zircon U−Pb geochronology and Hf isotopic compositions of the Mesozoic granites in southern Anhui Province, China[J]. Lithos, 150: 6−25

Wu Y B and Zheng Y F. 2004. Genesis of zircon and its constranints on interpretation of U− Pb age[J]. Chinese Science Bulletin, 49: 1554−1569.

Xie Jiancheng, Chen Si, Rong Wei, Li Quanzhong, Yang Xiaoyong, Sun Weidong. 2012. Geochronolgy, geochemistry and tectonic significance of Guniujiang A− type granite in Anhui Province[J]. Acta Petrologica Sinica, 28(12): 4007−4020.

Xing Guangfu, Hong Wentao, Zhang Xuehui, Zhao Xilin, Ban Yizhong, Xiao Fan. 2017. Yanshanian granitic magmatisms and their mineralizations in East China[J]. Acta Petrologica Sinica, 33 (5): 1571−1590 (in Chinese with English abstract).

Xue Huaimin. 2016. Geochronology, geochemistry and petrogenesis of volcanism in the Liyang volcanic basin on the southeastern margin of the Middle−Lower Yangtze region[J]. Geochimica, 45(3): 213− 234 (in Chinese with English abstract).

Xue Huaimin, Ma Fang, Guan Haiyan, Wang Yipeng. 2013. Geochronology and geochemistry of volcanic rocks in Huaining basin incomparison with other basins in the middle−lower Yangtze region[J]. Geology in China, 40(3): 694− 714 (in Chinese with English abstract).

Xue Huaimin, Wang Yinggeng, Ma Fang, Wang Cheng, Wang Deen, Zuo Yanlong. 2009. The Huangshan A− type granites with tetrad REE: constraints on Mesozoiclithospheric thinning of the southeastern Yangtze craton? [J]. Acta Geologica Sinica, 83(2), 247−259 (in Chinese with English abstract).

Yan Jun, Hou Tianjie, Wang Aiguo, Wang Deen, Zhang Dingyuan, Weng Wangfei, Liu Jianmin, Liu Xiaoqiang, Li Quanzhong. 2017. Comparative study of genesis of earlier−stage metallogenic granite and later− stage barren granite in the south Anhui Province[J]. Science China: Earth Sciences, 47(11): 1269−1291.

Yan Jun, Peng Ge, Liu Jianmin, Li Quanzhong, Chen Zhihong, Shi Lei, Liu Xiaoqiang, Jiang Zizhao. 2012. Petrogenesis of granites from Fanchang district, the Lower Yangtze region: Zircon geochronology and Hf−O isotopes constrains[J]. Acta Petrologica Sinica, 3209−3227 (in Chinese with English abstract).

Yang S Y, Jiang S Y, Zhao K D, Jiang Y H, Ling H F, Luo L. 2012. Geochronology, geochemistry and tectonic significance of two Early Cretaceous A− type granites in the Gan− Hang Belt, Southeast China[J]. Lithos,150: 155−70.

Zhang Bangtong, Zhai Jianping, Ling Hongfei. 1989. The geological and geochemical characteristcs of the mixed crust− mantle derivation type uranium− bearing granitoids in the lower Yangzi fault depression zone[J]. Uranium Geology, 5(3): 134− 143 (in Chinese with English abstract).

Zhang S B, He Q, Zheng Y F. 2015. Geochronological and geochemical evidence for the nature of the Dongling Complex in South China[J]. Precambrian Research, 256:17−20.

Zhang S B, Zheng Y F. 2013. Formation and evolution of Precambrian continental lithosphere in South China[J]. Gondwana Research, 23(7): 1241−1260.

Zhang S B, Zheng Y F, Wu Y B, Zhao Z F, Gao S, Wu F Y. 2006. Zircon isotope evidence for ≥3.5 Ga continental crust in the Yangtze craton of China[J]. Precambrian Research, 146:16−34.

Zhou J, Jiang Y H, Xing G F, Zeng Y, Ge W Y. 2013. Geochronology and petrogenesis of Cretaceous A− type granites from the NE Jiangnan Orogen, SE China[J]. International Geology Review, 55: 1359−1383.

Zhou Jie, Jiang Yaohui, Zeng Yong, Ge Weiya. 2013. Zircon U−Pb age and Sr, Nd, Hf isotope geochemistry of Jingde pluton ineastern Jiangnan orogen, South China[J]. Geology in China, 40(5): 1379−1391 (in Chinese with English abstract).

Zhou Taofa, Fan Yu, Yuan Feng. 2008. Advanees on petrogesnis and metallogeny study of the mineralization belt of the Middle and Lower Reaches of the Yangtze River area[J]. Acta Petrologica Sinica, 24(8): 1665−1678 (in Chinese with English abstract).

Zhou Xiang, Yu Xinqi, Yang Heming, Wang Deen, Du Yudiao, Ke Hongbiao. 2012. Petrogenesis and geochronology of the high Ba−Sr Kaobeijian granodiorite porphyry, Jixi County, south Anhui Province[J]. Acta Petrologica Sinica, 28(10): 3403− 3417 (in Chinese with English abstract).

Zhou X M, Li W X. 2000. Origin of Late Mesozoic igneous rocks in southeastern China: Implications for lithosphere subduction and underplating of mafic magmas[J]. Tectonophysics, 326 (3−4): 269−287.

Zhou X M, Sun T, Shen W Z, Shu L S. 2006. Petrogenesis of Mesozoic granitoids and volcanic rocks in South China: A response to tectonic evolution[J]. Episodes, 29(1): 26−33.

附中文参考文献

常印佛, 董树文. 1996. 论中—下扬子"一盖多底"格局与演化[J]. 火山地质与矿产, 17(1/2): 1−15.

陈芳, 王登红, 杜建国, 许卫, 胡海风, 王克友, 余有林, 汤金来. 2014. 安徽宁国刘村二长花岗地球化学特征、LA−ICP−MS 锆石 U−Pb 年龄及其地质意义[J]. 地质学报, 88(5): 869−882.

陈俊, 王辉, 王丽娟, 关俊朋. 2018. 滁州地区金牛侵入体的岩石成因：拆沉下地壳熔融还是壳幔混合[J]. 中国地质, 45(1): 110−128.

高冉, 闫峻, 李全忠, 刘晓强, 王思诺. 2017. 皖南谭山岩体成因：年代学和地球化学制约[J]. 高校地质学报, 23(2): 227−243.

关俊朋, 韦福彪, 孙国曦, 黄建平, 王丽娟. 2015. 宁镇中段中酸性侵入岩锆石 U−Pb 年龄及其岩石成矿指示意义[J]. 大地构造与成矿学, 39(2): 344−354.

侯可军, 李延河, 田有荣. 2009. LA−MC−ICPMS 锆石微区原位 U−Pb 定年技术[J]. 矿床地质, 28(4): 481−492.

凌文黎, 高山, 郑海飞, 周炼, 赵祖斌. 1998. 扬子克拉通黄陵地区崆岭杂岩 Sm−Nd 同位素地质年代学研究[J]. 科学通报, 43(1): 86−89.

吕庆田, 孟贵祥, 严加永, 张昆, 赵金花, 龚雪婧. 2019. 成矿系统的多尺度探测：概念与进展——以长江中下游成矿带为例[J]. 中国地质, 46(4): 673−689.

毛景文, Holly S, 杜安道, 周涛发, 梅燕雄, 李永峰, 藏文栓, 李进文. 2004. 长江中下游地区铜金(钼)矿 Re−Os 年龄测定及其对成矿作用的指示[J]. 地质学报, 78(1): 121−131.

王存智, 黄志忠, 赵希林, 褚平利, 黄文成, 宋世明, 陈志洪. 2018. 长江中下游宣城水东地区早白垩世酸性火山岩年代学、地球化学及岩石成因[J]. 岩石矿物学杂志, 37(5): 697−715.

王继强, 孙维安, 袁峰, 尚世贵, 周涛发, 钟富明, 张若飞. 2017. 庐枞盆地大倪庄铜矿床地质特征、成岩时代及成因探讨[J]. 中国地质, 44(1): 86− 100.

谢建成, 陈思, 荣伟, 李全忠, 杨晓勇, 孙卫东. 2012. 安徽牯牛降 A 型花岗岩的年代学、地球化学和构造意义[J]. 岩石学报, 28(12): 4007−4020.

邢光福, 洪文涛, 张雪辉, 赵希林, 班宜忠, 肖凡. 2017. 华东地区燕山期花岗质岩浆与成矿作用关系研究[J]. 岩石学报, 33(5): 1571−1590.

薛怀民. 2016. 长江中下游火山岩带东南缘溧阳盆地火山作用的年代学、地球化学及岩浆成因探讨[J]. 地球化学, 45(3): 213−234.

薛怀民, 马芳, 关海燕, 王一鹏. 2013. 怀宁盆地火山岩的年代学、地球化学及与长江中下游其他火山岩盆地的对比[J]. 中国地质, 40(3): 694−714.

薛怀民, 汪应庚, 马芳, 汪诚, 王德恩, 左延龙. 2009. 高度演化的黄山 A 型花岗岩：对扬子克拉通东南部中生代岩石圈减薄的约束？[J]. 地质学报, 83(2), 247−259.

闫峻, 后田结, 王爱国, 王德恩, 张定源, 翁望飞, 刘建敏, 刘晓强, 李全忠. 2017. 皖南中生代早期成矿和晚期非成矿花岗岩成因对比[J]. 中国科学: 地球科学, 47(11): 1269−1291.

闫峻, 彭戈, 刘建敏, 李全忠, 陈志洪, 史磊, 刘晓强, 姜子朝. 2012. 下扬子繁昌地区花岗岩成因:锆石年代学和 Hf−O 同位素制约[J]. 岩石学报, 28(10): 3209−3227.

章邦桐, 翟建平, 凌洪飞. 1989. 扬子断陷带中壳幔混源型产铀花岗岩的地质地球化学特征[J]. 铀矿地质, 5(3): 134−143.

周洁, 姜耀辉, 曾勇, 葛伟亚. 2013. 江南造山带东段旌德岩体锆石 LA−ICPMS 年龄和 Nd−Sr−Hf 同位素地球化学[J]. 中国地质, 40(5): 1379−1391.

周涛发, 范裕, 袁峰. 2008. 长江中下游成矿带成岩成矿作用研究进展[J]. 岩石学报, 24(8): 1665−1678.

周翔, 余心起, 杨赫鸣, 王德恩, 杜玉雕, 柯宏飙. 2012. 皖南绩溪县靠背尖高 Ba−Sr 花岗闪长斑岩年代学及其成因[J]. 岩石学报, 28(10): 3403−3417.